 CMES, vol.3, no.4, pp.417-429, 2002

Virtual Tribology: Integrating Model-Based Simulations with Modern Computation/Information Technologies

Q. Jane Wang[1], Michael D. Bryant[2], Leon M. Keer[1], and Richard F. Salant[3]

Preface

Modern computation and information technologies can greatly assist engineers in time compression of designs by developing "virtual" systems through simulations and cross-disciplinary integration. Virtual Tribology is a methodology for creating and analyzing elements and systems based on surface phenomena by means of integrating advanced model-based simulations with modern information technologies. Increasingly strong research attention is being directed to this area, which tends to merge into the stream of industrial computer-aided design and engineering.

The first Virtual Tribology Symposium was held on August 1, 2001 in Dearborn, MI, as a part of the Sixth U.S. National Congress on Computational Mechanics (USNCCM). The symposium was sponsored by the U.S. Association for Computational Mechanics (USACM) and the Co-Center for Surface Engineering and Tribology at Northwestern University and Georgia Institute of Technology. The symposium's intent was to bridge the fundamental research and method development with industrial applications and promote collaborations between researchers and engineers. It brought together tribologists in this new field, to facilitate communication among various practices of simulation and virtualization of tribological systems. It provided a forum to report research achievements and progress in this area, address key issues, discuss problems, and exchange experiences. Some of the papers presented in the symposium are further reviewed and published in this special issue of *Computer Modeling in Engineering & Sciences*.

Virtual tribology and concomitant development of virtual tribology systems may bring new technologies to industries. For example, new materials and emerging engineering technologies suggest many promising developments and challenges for powertrains, the power-delivery system of modern vehicles. By evaluating each material, coating and surface treatment with a traditional approach, industries may lose their competitive advantage unless development time can be reduced. Virtual tribology systems based on multi-scale simulations and cross-disciplinary integration can help compress the design cycle through rapid virtual evaluation. Modern computer technologies, together with advances in computational methods, can greatly save the time for developing "virtual" systems. We envision the virtual tribology systems to include (in its database) the latest technologies from materials science through simultaneous development, testing and modeling. Future designers may conduct 80-90% of "virtual tests" by computer through model-based simulations. We believe that the virtual-tribology concept will become important to future machine design and that the interface virtualization technology will become a core technology for the development of the surface pairs for the components of future machinery.

Existing virtualization tools for industries are mainly CAD-based solid modeling and mechanics-based analysis systems. An effective module to simulate the interactions of element surfaces in relative motion does not yet exist. Interfacial phenomena between contacting surfaces has been long recognized as being very complicated, involving interactions between two or three solids, or among solid, liquid and gas phases. The surfaces may fail due to single or combined failure mechanisms. Evaluating interactive surfaces and new materials requires tribological modeling of surface failure mechanisms, including material failure criteria and failure transitions. Model development and model-based simulations appear to be the keys to future virtual tribology systems. Considerable effort has been expended to develop such modeling, to bridge modeling and industrial tests and to increase the understanding of the many phenomena associated with contacting bodies and the competitive failure

[1] Northwestern University
[2] The University of Texas
[3] Georgia Institute of Technology

mechanisms involved.

Developments in simulating tribological systems are being made concurrently with the development of model-based simulations. This preface describes the state of the art developments in the description and simulation of surface contact interactions, and modeling and simulation of tribological components and systems.

1 Surface interactions and contact simulations

Power and motion of mechanical systems are transmitted though the contact and interaction of engineering surfaces. Contact simulation is the numerical process that determines the response of surfaces to a set of operating conditions, from which contact pressure and contact area are correlated with the normal separation of the contacting elements and, most importantly, with the material properties and surface roughness characteristics. Contact mechanics (Johnson 1996 and Ling 1973) lays a solid foundation for contact simulation research. A few papers reviewed the recent advances in analyzing and simulating the contacts between rough surfaces (Liu et al 1999, Barber and Ciavarella 2000, Tichy and Meyer 2000).

1.1 Surface description

The mathematical description of engineering surfaces is the first step toward modeling the contact between rough surfaces. Four methods, surface statistics, fractal characterization, numerical generation, and digitization, are commonly used for rough surface description. The statistical method provides a means to reflect the random nature of the rough surface, in which stochastic analysis processes are combined with surface measurements. The major advantage of this method of the rough surface description is its simplicity and explicitness in expressions, which greatly facilities derivations of closed-form contact equations and fast contact analyses. Many advances have been made since the pioneering work by Greenwood and Williamson (1965), Greenwood and Tripp (1971), Whitehouse and Archard (1970). With the statistical method, surfaces may be described by a height distribution function and the characteristics of the distribution functions. Usually, the shape of asperities needs to be specified in order to use the existing contact formula for contact analyses. Spherical and parabolic tip shapes, as well as cylindrical asperities, are commonly adopted. In most of the descriptions, asperity heights were assumed to follow the Gaussian distribution with respect to a mean plane. Generally, a few parameters, such as the standard deviation of the asperity height distribution, the density of asperities per unit area, and the radius of curvature of asperities, and sometimes, the correlation distance, need to be acquired for modeling. Fractal characterization of surfaces aims at quantifying the multiscale nature of surface asperities with scale-invariant fractal parameters. Contact models that utilize the theory of fractal geometry have been developed recently (see Majumdar and Bhusan 1991, Borodich and Onishchenko 1997). The major parameters used for the roughness characterization are the ones that reflect the distribution of the frequency numbers of a surface and the amplitude of variations at all frequency numbers. The fractal analyses of surfaces may retain the roughness structural information and can yield scale-independent surface parameters to be used for pressure and deformation calculations. Surfaces may also be numerically generated based on a few measured statistical parameters. Patir (1986) presented a numerical method of rough surface generation that was later used in many studies. His procedure can produce a three-dimensional surface profile based on the Gaussian distribution of the asperity height $z(x, y)$ and a bilinear autocorrelation function $R(\lambda_x, \lambda_y)$. The digital-filtration technique is also used for a 3-D rough surface generation with a given standard height deviation and an autocorrelation function (Hu and Tonder 1992). With this technique, the heights of a rough surface are considered as signals of a time-dependent series of a random process, and the 3-D random surface is generated through a linear transformation of a series of random input signals. Recently, the surface generation technique is combined with a neural-network process for predicting and re-producing worn surfaces in a wear process (Ao et al. 2002). Direct digitization of real surfaces should render the most realistic description of the surface topography. A few types of instruments are currently available for measuring the surface topography, such as the stylus-type surface profilometer, the optical (white-light interference, for example) measurement instrument, and the atomic Force Microscope (AFM). Among them, the first two instruments are usually used for macro-to-micro asperity measurements, whereas AFM may be used for micro- or nano-scale problems.

1.2 Contact-simulation models

Many contact-simulation models have been developed and applied to the tribological research of machine components. The major effort of contact simulation is on the isothermal analysis of contact between rough surfaces. The Hertzian solution is used for the contact of rough surfaces if the shapes and radii of asperities are prescribed. With the Hertzian solution, one can obtain the expression for the normal load and contact area for each asperity without considering the asperity interaction. The Flamant and Boussinesq formulas, or their alternatives, for the relationship between displacement and contact pressure are widely used in two-dimensional (Flamant) and three-dimensional (Boussinesq) elastic contact problems. For two elastic bodies in contact, the composite surface displacement is usually obtained through replacing $E/1-\nu^2$ by the composite Young's modulus, *E'*, *from* $\frac{1}{E'} = \frac{1-\nu_1^2}{E_1} + \frac{1-\nu_2^2}{E_2}$ (Johnson 1996). Then, the contact inequalities (deformed asperities are either in contact, with positive pressure, or not in contact, with positive gap) are solved through iterative solution processes. Typically, contact solvers divide the contact domain into small elements, and so the contact pressure can be treated as a constant on each element. The large number of elements needed to capture the contact of rough surfaces led to the use of multi-level multi-summation and conjugate gradient techniques to increase the speed of each calculation at each iterative step and to increase the speed and convergence of the overall iteration (Lubrecht and Ioannides 1991, Polonsky and Keer 1999).

The fast Fourier transform (FFT) and inverse fast Fourier transform (IFFT) are now intensively utilized to reduce the computational burden in solving contact problems. The continuous convolution and Fourier transform (CC-FT) algorithm uses the continuous convolution theorem and frequency response functions to formulate the problem in the frequency domain. FFT and IFFT are applied to replace the Fourier transform and inverse Fourier transform, respectively. Here, spatial fields may be interpreted to be periodic. Three methods have been developed to improve the accuracy (i.e. to diminish the periodicity error) of the CC-FT algorithm, namely, the domain-extension method (Ju and Farris 1996), the traction decomposition method (Ai and Sawamiphakdi 1999), and the error compensation method (Polonsky and Keer 2000 a and b). With the domain-extension method, the dimension of the computation domain for displacement calculation is extended many (8 or more, as Ju and Farris (1996) recommended) times that of the original problem. With the traction decomposition method, the traction is resolved into a smooth part and a zero-mean fluctuating part. The response to the smooth part is known analytically and the CC-FT algorithm is needed only for the fluctuating part. With the error compensation method, a hybrid algorithm is constructed by adding a special correction procedure based on the multi-level multi-summation technique. Alternatively, the discrete convolution and fast Fourier transform (DC-FFT) algorithm (Liu et al 2000) uses the discrete convolution theorem, FFT, IFFT, and the influence coefficients, with the processes of zero padding and wrap-around order, to completely avoid any FFT- or IFFT- related error at a cost of only doubling the domain dimensions of a contact problem. This DC-FFT algorithm makes the FFT technique satisfactorily applicable to elasticity and thermoelasticity problems (Liu and Wang 2001). The DC-FFT algorithm requires influence coefficients, which can often be found analytically. If the frequency response functions are known instead of the influence coefficients, such as in the more complicated problems of layered materials in contact, the DC-FFT algorithm can be applied with influence coefficients found from the frequency response functions (Liu et al 2000) in a preprocess similar to that in the CC-FT algorithm with a sufficient domain extension (see also Nogi and Kato 1997). Once the conversion to influence coefficients is accurately accomplished, no additional periodicity error is expected in the DC-FFT algorithm. Now, the FFT technique has been applied to solving elasto-plastic problems in contact, as demonstrated by Sainsot et al. (2002) in this issue.

1.3 Flash temperature and thermoelastic contact analysis

Frictional heating of rough surfaces is inevitable in tribological contacts and is often responsible for failures, such as scuffing, seizure, and cracking. The thermal information regarding contacts is necessary for studies of the interfacial activities in a tribological process. Carslaw and Jaeger's Conduction of Heat in Solids (1959) provides basic equations and methods for the temperature analysis. Two approaches, decoupled thermal-elastic approach and coupled thermal-elastic approach, are now used for the flash-temperature analysis in contact. With

the former, an isothermal contact problem is analyzed first to obtain the asperity-contact pressure, and a heat-transfer problem is then solved separately, where the heat input is determined based on the contact-pressure information. With the latter, coupled contact, heat transfer and thermoelastic problems are solved interactively where the influence of asperity thermoelastic distortion is taken into account.

Frictionally excited thermal instability is another important aspect of thermally-related contact analyses. It has been found that the thermoelastic distortion due to frictional heating can initiate an unstable feedback process, that is, the distortion causes the contact pressure to increase, which in turn further enhances the distortion. Time-dependent heat-transfer equations could be incorporated in contact models where the pressure, contact area, and deformations are all considered temperature dependent. The studies of a single asperity and a halfspace with a known pressure distribution (Huang and Ju 1985, Ting and Winer 1989) revealed basic thermomechanical phenomena of contact subjected to frictional heating. The fundamental thermoelastic analyses with a given heat source on a halfspace developed basic analytical tools and methods for thermoelastic contact simulation. Recently, thermomechanical models for rough surfaces in contact and rubbing are reported, simultaneously considering the thermal phenomena (heat transfer and the thermoelastic behavior), the mechanical response (elastic-perfectly-plastic behavior), and the interaction (the contact constraints). Two thermoelasticity-related papers are included in this issue (Liu et al 2002 and Rodgers et al. 2002). The latter describes steady-state flash-temperature while the former analyzes transient thermoelastic deformations.

2 Modeling and simulation of tribological components

Tribological components may be largely classified as conformal-contact elements, such as journal bearings and most seals, and counterformal elements, such as gears and rolling-element bearings. Due to the nature of contact and relative motion, these groups of elements may operate under different interfacial conditions and face different failure mechanisms. Conformal contact may occur on a large area of interaction, and modeling these elements requires the analysis of on entire structure. Counterformal-contact elements commonly work under cyclic stresses and highly localized deformation. They are usually treated as half planes or halfspaces in analyses.

2.1 Journal-bearing conformal contact

Journal bearings are widely used in engineering equipment to transmit radial load. Usually, journal bearings are dynamically loaded. Full-film hydrodynamic lubrication is the desired lubrication status a journal bearing should be designed with. However, the trend of compact and energy-saving designs tends to push journal bearings to work in the regime beyond the full-film lubrication. In general, modeling journal-bearing lubrication requires interactive solutions to the Reynolds equation that governs the flow hydrodynamics, the energy equation that describes the system heat transfer, and the elastic equation that takes into account the material response to a group of operating conditions. Hydrodynamics and thermohydrodynamics of conformal contact elements like journal bearings are well described by Pinkus and Sternlicht (1961) for the former and Pinkus (1990) for the latter. Modeling and simulation of the performance of journal bearings may be classified as hydrodynamic (HD), elastohydrodynamic (EHD), thermohydrodynamic (THD) and thermo- elastohydrodynamic (TEHD) for bearings in full-film lubrication, and mixed-TEHD for those working under severe operating conditions. With the assistance of the power of modern computers, researchers are able to tackle more complicated problems, either in geometry or in hydrodynamics. A few of such examples are included in this issue (Jang and Khonsari 2002, Shi and Paranjpe 2002, and Wang et al, 2002).

In modeling conformal-contact lubrication, one needs to consider the fact that the size of the contact region may be in the same order of magnitude as that of the contacting bodies. Applications of the Boussinesq type of formulation, which is based on a half space, to solve conformal contact elasticity would introduce a significant inaccuracy. Woodward and Paul (1976) formulated a general numerical method in terms of influence functions that use modified Green's functions to solve conformal contact problems. More complete solutions for structures with complicated finite conformal geometry rely on the finite element method (FEM).

Journal-bearing conformal contacts may fail due to scuffing and seizure. Seizure is a catastrophic failure of tribo-

logical systems, which may be considered as stopping of relative motion due to material interlocking. Although seizure is observed, generally speaking, in both non-conformal and conformal contacts, it is more likely to happen in the latter, particularly in journal-bearing conformal contacts. It seems that conformal contacts are more sensitive to geometric changes, local and global; and seizure failure is more closely related to increases in both of the interfacial flash temperature and the overall temperature of contacting elements. Major causes of seizure of journal bearings may fall into the following categories: (1) loss of clearance due to differential thermal expansions of the journal and bearing, (2) loss of clearance due to building-up of wear debris, (3) intimate metal-metal contacts, and (4) variation of surface geometry and material properties due to interfacial tribochemical activities.

In journal-bearing lubrication, scuffing is usually considered to be the stage leading to seizure. Predicting scuffing failure directly help avoid seizure to occur. Studies of scuffing failure of sliding contacts in the 70's and early 80's were focused on the macro-scale parameters that controlled the failure processes, and the results were presented in the form of transition diagrams governed by the load and speed relationship. However, the recent trends of research tend to discover detailed interfacial phenomena in micro-scale contacts by considering the mechanical, physical, and chemical interactions. A dynamic model of scuffing for automobile engine applications developed by Hu et al (2002) included in this issue is one of the examples of such efforts.

2.2 Mechanical Seals

The mechanical seal is an example of a tribological component for which the methods of virtual tribology have significantly transformed the design process. Although mechanical seals have been in use since the early part of the 20^{th} century, until the 1990's they were designed using largely empirical methods. The only tools the designer had available were his/her previous experience, rule of thumb methods and the test laboratory. This situation began to change in the 1990's as a result of research begun in the late 1970's and early 1980's.

Mechanical seals are precision devices that are essential components in such turbomachines as pumps and compressors. They also happen to be one of the machine components most prone to failure. The low reliability and short life of mechanical seals induced users and manufacturers to seek more effective seal designs through the development of better and more sophisticated design methods. This led to the earliest numerical models of mechanical seals in the late 1970's and early 1980's. These models primarily dealt with liquid lubricated non-contacting pump seals operating at steady state. Such seals were of major interest because the existence of a continuous lubricating film between the seal faces was believed to increase reliability and life. However, in sealing hydrocarbons, these seals became unstable when the liquid lubricating film partially vaporized. This led to the development of unsteady two-phase models of non-contacting seals. In addition, at this time there was some limited modeling of contacting mechanical seals, totally ignoring the presence of a fluid lubricant, because of applications involving very heavily loaded unbalanced seals, such as automotive water pump seals.

In the 1990's, government regulations limiting seal emissions led to the need for seals with thinner and thinner lubricating films, so that seals operating with asperity contact became more common. This resulted in contacting seal models that account for mixed lubrication between the seal faces. Another important development in the 1990's was the development of so-called "dry gas seals" for both gas sealing applications (compressors) and liquid sealing applications (pumps). These utilize faces containing etched patterns, such as spiral grooves, and therefore resulted in the construction of hydrodynamic gas seal models. The use of mechanical seals in high speed compressors also lead to a heightened interest in mechanical seal dynamics, since the seal stiffness and damping characteristics play important roles in the machine rotor dynamics. While the fundamentals of mechanical seal dynamics were established in the 1980's, the higher shaft speeds led to further dynamic model enhancement. Perhaps the most important development in the 1990's was the shift of mechanical seal models from the research stage to their use as a design tool. Today, at the beginning of the 21^{st} century, every major mechanical seal manufacturer uses some form of virtual tribological seal model in the development of new designs, as well as in the troubleshooting of current designs.

2.3 Rotary Lip Seals

The rotary lip seal is another important tribological component for which the methods of virtual tribology are ap-

propriate. These seals are mass produced products, extensively used in the automotive, appliance and industrial machinery industries. Like mechanical seals, lip seals first came into use in the early 20^{th} century. However, unlike the situation with mechanical seals, there is no virtual tribological lip seal model suitable for use as a design tool, currently available. The virtual tribology of rotary lip seals is about ten years behind that of mechanical seals.

There are several similarities between lip seals and mechanical seals. Both operate with a micron-scale lubricating film between the sealing surfaces, and both contain a self-adjusting, deformable and moveable surface. Thus the analyses of both involve a problem in elastohydrodynamics. However, there is also a very important difference between the two types of seals. While the mechanical seal's operation is primarily dependent on the macroscopic characteristics of the seal, the lip seal's operation is strongly dependent on the microstructure of the rubber surface under the lip. The shape and size distribution of the microasperities, and the manner in which the microasperities deform, play dominant roles in determining the behavior of the seal. The complexity of the physical processes (which do not occur in mechanical seals) and the computational difficulties in simulating them are what have retarded the development of useful numerical lip seal models.

Although serious experimental studies of rotary lip seals began in the 1950's, it was many years before even a rudimentary understanding of the important physical processes was obtained. Therefore, it was not until the early 1990's that attempts to construct numerical lip seal models were made. Over the last decade these models have become more sophisticated, and have been extremely successful in elucidating the physics of lip seal operation. However, since these models simulate microscale processes over macro-scale configurations using a deterministic approach, they require very large computation times. While such models are very useful for research purposes, their utility as design tools is extremely limited, so that lip-seal manufacturers currently rely exclusively on empirical means to design their seals. To overcome this problem, efforts are now directed toward constructing lip seal models using a statistical approach, which has the potential of greatly reducing computation time and yielding a practical design tool.

2.4 Mixed lubrication

The understanding of lubricated interfaces rely on modeling and simulation of surfaces under mixed lubrication. Classic lubrication theories and contact mechanics have laid a strong foundation for mixed-lubrication research. Since the stochastic lubrication models by Christensen (1970) and Patir and Cheng (1978), many studies on the mixed lubrication of conformal-contact elements have been conducted. Generally, three approaches have been used in the mixed-lubrication studies on either conformal or counterformal contact: (1) deterministic modeling that desctitizes governing equations based on three-dimensional rough surfaces, (2) stochastic modeling that aims at developing average flow models, and (3) interactive deterministic-stochastic modeling that applies the average flow models to solve bearing mixed lubrication problems. Stochastic models use selected statistic parameters to represent the influence of roughness on lubrication. They are powerful in drawing general features and handling problems that are large in size. Average flow models have been proven effective in the studies of some conformal-contact problems where the asperity contacts are localized in a few characteristic regions. In interactive deterministic-stochastic modeling, lubrication is processed through the macro-scale average flow model while the contact is calculated by means of an off-line deterministic asperity contact model. This method is evolving to solve more problems, including the mixed lubrication of counterformal-contact elements. Realistic deterministic models link the surface tribological performance to materials and surface design, and provide a solid base for other related research (See Zhu and Hu (2001)). The major part of frictional heat in mixed lubrication may be generated in rubbing asperities in contact. So far, macro-scale thermal studies involving micro heat source analyses are available for conformal interfaces, where asperity contact is either ignored or averaged over the size of an element of a computational mesh.

2.5 Fatigue and wear

Most counterformal contact elements, such as gears and rolling-element bearings, are subjected to cyclic and concentrated contact pressure that may lead to rolling contact fatigue (RCF). Fatigue and wear are two interactive damage mechanisms that affect the life of components in relative motion. The gradual evolution of system parameters caused by repeated rolling/sliding contact should be

taken into account when modeling coated surfaces. In particular, the gradual change in the coating thickness due to various mild wear modes needs to be integrated into both crack initiation and crack propagation models. Gradual wear is a crucial issue for many important applications, from mechanical seals to gears. Hence, a new coating structure maximizing the coating toughness will not be acceptable if it also results in a significant loss of the resistance to mild wear. In such a case, the coating may not fail catastrophically, but it will be polished off quickly and will not be able to protect the substrate.

Efforts to understand fatigue and wear require physics-based models rooted in deformation and fracture in the microstructures of nanolayered coating/substrate systems. Some understanding of microstructure related failure mechanisms and the pioneering work has already been achieved. The contact fatigue life models commonly in use today assume that the pitting life is controlled by fatigue crack initiation, and neglect the crack propagation portion of fatigue life (Ioannides and Harris, 1985, Zaretsky et al., 1996, Ai 1998). Such theories are adequate for rolling bearings, but they may be restrictive for predicting pitting in gears. Experimental evidence suggests that the pitting life under rolling/sliding conditions is controlled by crack propagation, and that the lubricant entrapment in the crack plays a crucial role (Murakami, et al. 1997), which confirms the classical results of Way (1935). Further modeling work recognizes that a number of different physical mechanisms can control the pitting life of a coated gear surface, depending on the material combination and the operating conditions.

In many practical situations the life may be controlled by fatigue crack propagation, within the coating or in the substrate. Coating microstructure effects are studied systematically and quantitatively first. There have not been any systematic, accurate analyses of the coating microstructure effect on its toughness. Although a number of multilayer and nanocomposite coatings having improved toughness and contact fatigue resistance have been developed in the last few years (Voevodin and Zabinski 1998) there seems to be no clear understanding about how they work. It is necessary to understand exactly why and when such crack deviation makes the coating tougher. An ability to predict which combinations of microstructural elements may be effective has been initiated through fracture studies of layered coatings by Polonsky and Keer (2001, 2002). Those studies give a more precise local description of the contact stress field for the coating, which is typically complex and non-uniform. The type of loading was found to have a profound effect on the crack propagation mode, crack path, and the observed coating toughness.

3 Modeling and simulation of tribological systems

Tribological systems, wherein two surfaces mechanically interact, are critical to machinery. Transmission of mechanical power invariably involves some form of contact and inter-body motion between neighboring components. Successful designs are critically dependent on a-priori knowledge of the boundary loads and motions imposed onto the surfaces by the rest of the machine. Prediction of component service lives due to deterioration—including wear and fatigue–depends on accurate estimates of boundary loads and their cyclic variations. Consequently, designs must account for behavior between the machine system and the tribological components.

Most *real* machines and components—helicopters, vehicles, gearboxes, motors, pumps, turbines–are dynamic systems with many degrees of freedom, high dynamic orders, and mixtures of components: bearings, gears, seals, shafts, motors, and electronics, among others. Accurate codes predict bearing forces and deflections, shaft deformations, seal leakage, and motor torque. Usually these codes are self-contained modules, and treat the rest of the system as boundary conditions. This forces machine system designers to perform system simulations in pieces, and patch pieces together. To insure consistency of loads and motions, the procedure must iterate back and forth between modules. This cumbersome iterative scheme can be inaccurate, inefficient, and may not converge.

Modeling should treat the system as an integrated whole. Methods include direct application of fundamental physical laws, transfer functions, and energy-based methods such as bond graphs. Direct application of physical laws for very large-scale systems is complicated by vector mechanics and conversion factors between very different system physics (electric, magnetic, rigid body mechanics, solids, fluids, etc.). Transfer functions which map flow of signal through a system can suffer from incomplete causal (cause and effect) relations, and may violate conservation of energy. Bond graphs can guide modeling of complicated systems such as gear boxes, electric motors, hydraulics, vehicle drive trains, and actuators, among others. Bond graphs (Karnopp et al. 2000), in-

vented by Paynter (1960) abstracts any physical system into an "equivalent circuit" and maps power and energy flows through the system. Power P is the product of an effort e times a flow f ($P = ef$): voltage V times current i for an electrical system ($P = Vi$); force F times velocity v for a mechanical system ($P = Fv$); torque T times angular velocity ω for a rotational system ($P = T\,\omega$); pressure p times volumetric flow rate u for a fluidic system ($P = pu$); and magneto-motive force M times magnetic flux rate $d\phi/dt$ for a magnetic system ($P = M\,d\phi/dt$). For any element in any system, the difference between power flowing in P_{in} and power flowing out P_{out}, must equal the sum of the power stored P_{stored} (as energy) and dissipated P_{lost} :

$$P_{\text{in}} - P_{\text{out}} - P_{\text{stored}} - P_{\text{lost}} = 0 \tag{1}$$

Figure 1a shows an RLC series electrical circuit excited by a voltage source, and figure 1b shows a mass-spring damper mechanical system excited by an applied force. All elements of the circuit have the same current i, and all elements of the mechanical system have motions with the same velocity v. Both systems have sources of power—voltage source $V(t)$ and applied force $F(t)$, devices that store potential energy—capacitor C and spring k, devices that store kinetic energy—inductor L and mass M, and devices that dissipate power—resistor R and damper B. If one equates capacitor charge q and spring extension x, force F and voltage V, and current i and velocity v, the two systems will have the same differential equations. The bond graph of figure 1c maps power flows through the series RLC circuit and the mass-spring-damper system: Sources (effort S_e:e and flow S_f:f) bring external power to/from the system; capacitances (C:C) store potential energy; inertances (I:I) store kinetic energy; resistances (R:R) dissipate power; 0 and 1 junctions distribute power and simultaneously enforce a common flow or common effort constraint to all elements bonded to it; transformers (TF:n) and gyrators (GY:r) transform power to other forms. The symbol after the colon represents the parameter associated with the device. Bonds joining elements indicate interaction and exchange of power between these elements. Half arrows on bonds indicate the direction of positive power. In figure 1c, power originates from effort source S_e:F . Some power is stored in the capacitance of the spring compliance C:$1/k$ as potential energy, some power is stored in the inertia of the mass I:M as kinetic energy, and some power is dissipated by the resistance of the damper R:B. The "1 junc-

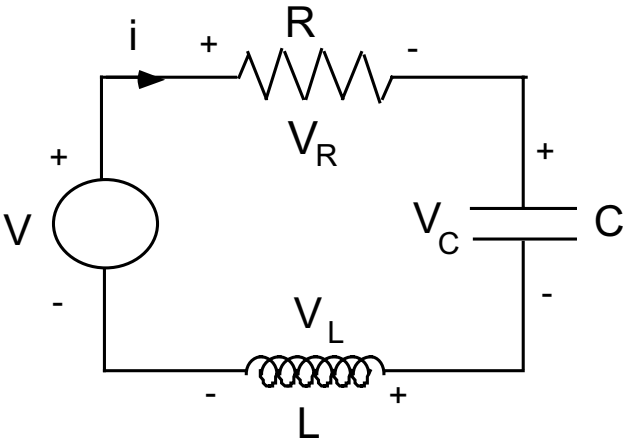

(a)

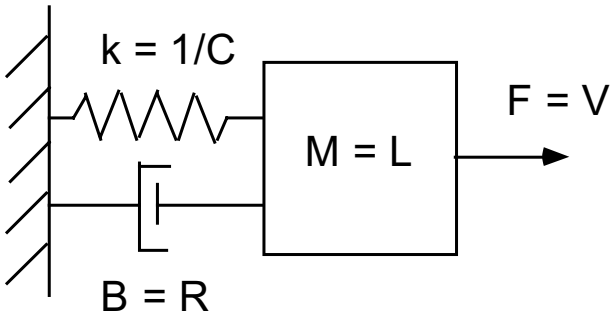

(b)

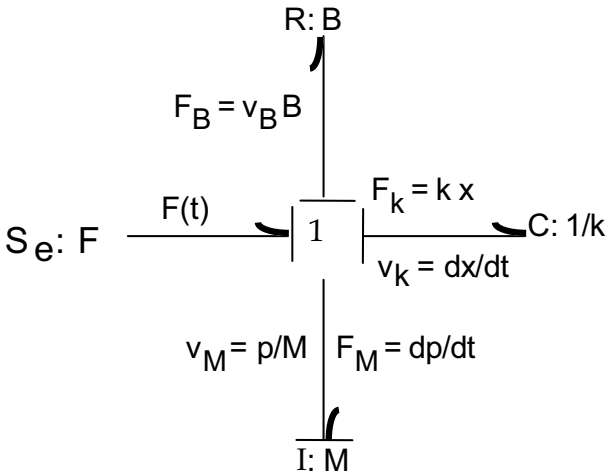

(c)

Figure 1 : (a) An RLC series circuit and a (b) mass-spring-damper produce (c) the same bond graph.

tion" distributes power from S_e:F to the other elements (C:$1/k$, I:M, R:B). and equates velocities. For the mass-spring-damper system of figure 1b, all elements move at the same velocity $v = v_M = v_k = v_B$, a kinematic consequence of their attachments. For the series circuit of figure 1a, this is tantamount to elements having the same current i. If the power balance of equation (1) is applied to these systems, the following equation results:

$$(F - F_B - F_k - F_M)v = 0 \tag{2}$$

For the mechanical system, the terms in parenthesis in equation (2) are equivalent to D'Alembert's dynamic equilibrium[4]. If voltage V should replace force F, the terms within the parenthesis become Kirchoff's voltage law, which tallies the voltage drops around the circuit.. From the power balances of equation (2) can arise state equations.

In addition to the above, each bond graph element has a constitutive law, and a cause and effect relationship to the rest of the system: together, these completely define that element's response. For example, the damper in figure 1b can have constitutive laws $F_B = v_B B$ or $v_B = F_B/B$ relating force F_B and extension velocity v_B . The causal stroke–the short line segment perpendicular to the bond—indicates which applies. For the bond joining the 1 junction and R:B, the causal stoke away from R:B indicates R:B accepts a velocity and responds with a force: thus $F_B = v_B B$ applies. The causal stroke on the bond joining C:$1/k$ to the 1 junction indicates C:$1/k$ accepts v_k = dx/dt, and "integrates" to get extension x. This renders spring constitutive law $F_k = kx$. (not x =F_k/k). The causal stroke on the bond joining I:M to the 1 junction indicates I:M accepts force F_M, from the 1 junction. Via physics for inertia, F_M = dp/dt and the mass "integrates" to get momentum p. The inertia has constitutive law $v_M = p/M$ relating mass velocity to momentum (not $p = Mv_M$). Labels for effort (found on the half arrow side of a bond) and flow (found on the non-half arrow side) on bonds indicates how elements behave. For example, the force $F_k = kx$ for the spring C:$1/k$ is labeled on the half arrow side of the bond in figure 1c.

If the constitutive laws are substituted into equation (2), and the kinematic relation $v_B = v_k$ = dx/dt = $v_M = p/M$ imposed by the 1 junction is invoked, the state equations of motion become

$$F - (\frac{p}{M})B - kx - \frac{dp}{dt} = 0, \qquad \frac{dx}{dt} = \frac{p}{M} \tag{3}$$

Figure 2a shows a parallel RLC circuit excited by a current source, and figure 2b shows a mass-spring-damper in mechanical series excited by an applied velocity. For these configurations, all elements share a common effort:

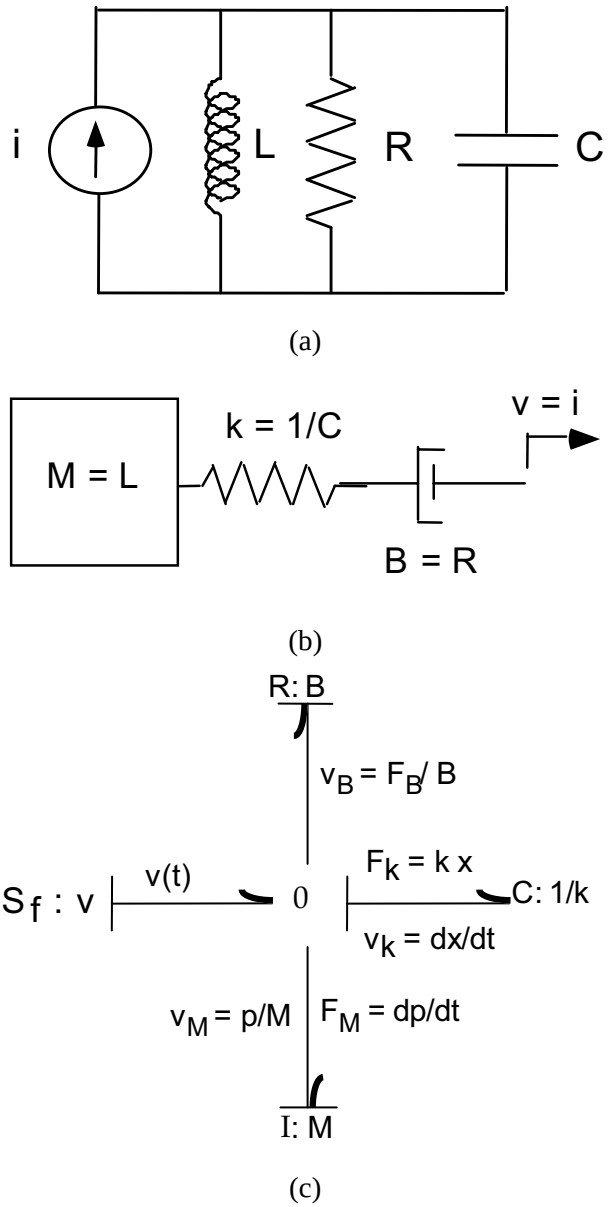

Figure 2 : (a) An RLC parallel circuit with current source and (b) a mass-spring-damper in series with prescribed velocity at ends produce (c) the same bond graph.

[4] Related to Newton's second law, wherein mass time acceleration is viewed as the inertial force.

the circuit elements in parallel have the same voltage V, and the mechanical elements connected in series experience the same force F (free body diagrams will confirm this). The arguments concerning balance of power are similar to those for figure 1. Here the "0 junction" in figure 2c distributes power from the flow source S_f:v to the other physical elements (C:$1/k$, I:M, R:B), with an auxiliary constraint of enforcing a common effort (same voltage V onto the parallel electrical elements, and same force $F = F_B = F_k = F_M$ onto the mechanical series elements). Equation (1) applied to figure 2c yields

$$(v - v_B - v_k - v_M)F = 0 \tag{4}$$

In light of constitutive laws and causality, equation (3) becomes

$$v - \frac{kx}{B} - \frac{p}{M} - \frac{dx}{dt} = 0, \qquad \frac{dp}{dt} = kx \tag{5}$$

Other elements are available for system model construction. Transformers TF:n with modulus n relate effort e_1 to effort e_2 and flow $f_1$to flow f_2 via $e_1 = ne_2$, and $f_2 = nf_1$. The transformer could represent the electrical transformer's step up of voltages $V_1 = nV_2$ and step down of currents $i_1 = n^{-1}i_2$, where n represents the turns ratio; the mechanical force advantage of levers $F_1 = nF_2$ with concomitant reduction of speed $v_1 = n^{-1}v_2$, where n represents the ratio of lever lengths; the torque increase $T_1 = nT_2$ of gears, with decrease in angular velocity $\omega_1 = n^{-1}\ \omega_2$, where n is the gear ratio; or for rollers on flats, the conversion of torque to force $T = RF$, and rotational speed to linear velocity $v = R\ \omega$, where modulus $n = R$ is the roller radius. Gyrators GY:r with modulus r relate efforts to flow $e_1 = rf_2$ and $e_2 = rf_1$. Gyrators can model current to torque production $T = ri$ of simple motors, with back emf $V = r\ \omega$ dependent on rotational speed, where r is the motor constant; or in coils wherein magneto-motive force is produced by current $M = ri$, with back emf $V = r\ d\phi/dt$ generated by rate of change in flux, where r is the number of coil turns.

Elements (C, I, R, TF, GY) can have multiple bonds bringing power in and out. Multiple port transformers can represent coordinate transformations, such as coordinate rotations or translations. Multi-port R, C, or I elements can represent fields: electrical, elastic, magnetic, fluid, etc. For example, deformation of bodies with distributed elasticity and mass can be estimated via the Finite Element method, wherein the body is divided into multiple elements with nodes having nodal displacements, and nodal forces that can depend on the nodal displacements, often through a stiffness matrix. Bond graphs can account for distributed mass, elasticity, and damping via multi-port energy storage elements—inertances and capacitances—and multi-port resistances joined together at 1 junctions. Here 1 junctions with common flows (velocities) record nodal velocities, the rate of change of nodal displacements, and FEM nodes manifest as bond graph 1 junctions.

Very complicated systems can be effectively modeled by linking together bond graph elements. Once the composite model has been assembled, systems of first order state equations similar to equations (2) and (4) can be extracted.

Consider a curved body with radius of curvature R contacting a flat. Hertz (Timoshenko and Goodier 1970) found a relation between contact force P and normal approach α as

$$\alpha = \left\{ 9\pi^2 P^2 \frac{(k_1 + k_2)^2}{16R)} \right\}^{1/3}, \qquad k_i = \frac{(1 - \nu_i^2)}{\pi E_i} \tag{6}$$

This displacement α to force P relation can be rearranged to give

$$P = C\alpha^{3/2}, \qquad C = \frac{4R^{1/2}}{3\pi(k_1 + k_2)} \tag{7}$$

The preceding defines a non-linear stiffness. If the sliding contact involves Coulomb friction, the friction force $F = \mu P$, where the direction of the force opposes the motion, and the coefficient of friction

$$\mu(v_s) = \mu_d + (\mu_s - \mu_d)\exp\{-v_s/v_0 \tag{8}$$

diminishes from its static value with static μ_s to its dynamic value μ_d as the sliding velocity v_s increases beyond and a critical velocity v_0. This defines a bond graph resistance with a force dependent on the sliding velocity through equation (7), and on the normal force P. Since the physics of the sliding contact couples effects of orthogonal motions (normal and tangential to the surface), we will combine these functions into a 2 - port RC element that has a capacitance character on one port, and a resistance character on the other port. The system layout is illustrated in figure 3a, and a bond graph showing the coupled dynamics between normal and tangential motions is shown in figure 3b. The state equations of

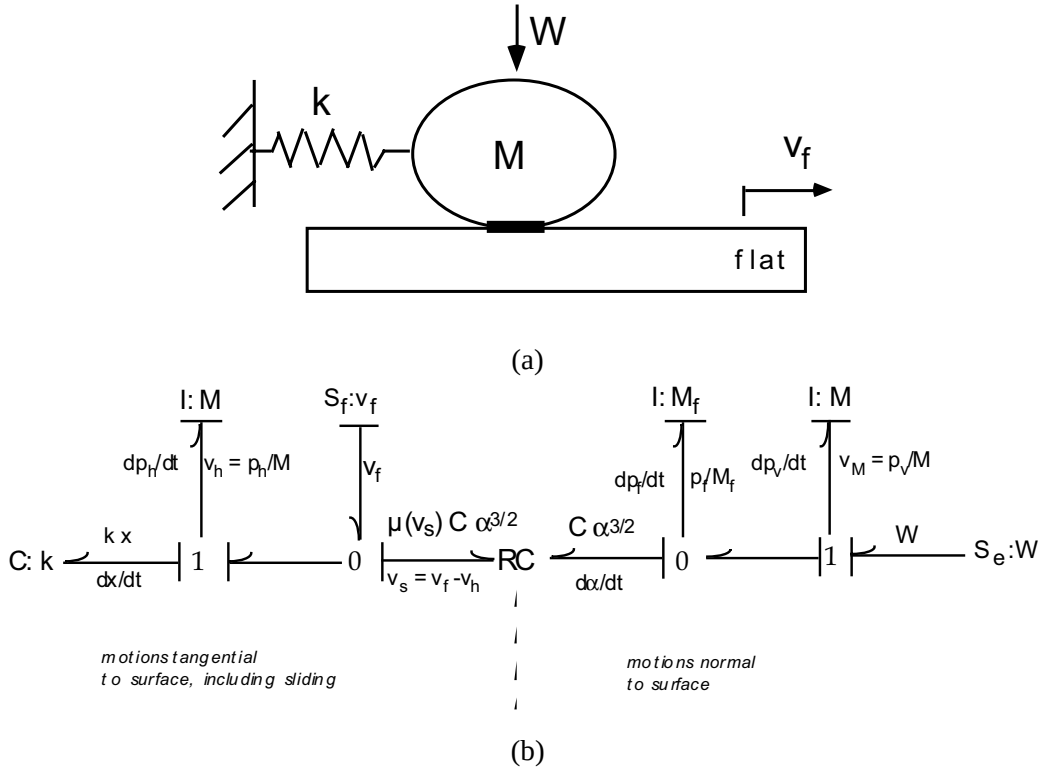

Figure 3 : (a) A sliding system consisting of curved body of mass M restrained by spring and pressed against a flat moving horizontally at velocity v_f with applied force W. (b) Bond graph of the sliding system of part a.

motion extracted from the bond graph are:

$$\begin{aligned}
\frac{dp_h}{dt} &= -kx + \mu(v_f - p_h/M)C\alpha^{3/2} \\
\frac{dx}{dt} &= p_h/M \\
\frac{dp_f}{dt} &= C\alpha^{3/2} \\
\frac{d\alpha}{dt} &= p_v/M - p_f/M_f \\
\frac{dp_v}{dt} &= W - C\alpha^{3/2}
\end{aligned} \tag{9}$$

The first and last equations originated from balancing efforts over the 1 junctions, i.e., enforcing D'Alembert's dynamic equilibrium principle associated with 1 junctions. The second arose from the common flow constraint of the left side 1 junction: equating the spring's extension rate to the mass velocity. The third arose from the common effort constraint of the right side 0 junction: here the normal contact force is the agent that compresses the contact. The fourth arose from the kinematic balance of velocities inherent in the right side 0 junction: this relates the rate of change of the normal approach between bodies to the velocities of the bodies. Finally, the velocity difference $v_s = v_f - p_h/M$ within the argument of the friction coefficient in the first equation was obtained by balancing the flows over the right side 0 junction.

With appropriate initial conditions, this system of equations can be solved to estimate contact vibrations incurred during sliding, such as stick-slip. These vibrations usually depend on other components in the physical system. These dependencies can be brought into the bond graph by replacing the sources S_f:v_f and S_e:W in figure 3b with other bond graph modules that represent those portions of the machine that produce the aforementioned loads.

State equations for far more complicated machine systems with tribological components can be formulated with bond graphs. An example—a gear box with three deformable shafts, bearings and gears appears in this issue (Choi et al 2002).

References

Ai, X.L., (1998): "Effect of three-dimensional random surface roughness on fatigue contact", *ASME Journal of Tribolog* **120**, 159.

Ai X.L., Sawamiphakdi, K., (1999): "Solving Elastic Contact Between Rough Surfaces as an Unconstrained Strain Energy Minimization by Using CGM and FFT Techniques," *ASME Journal of Tribology*, **121**, pp.639 - 647.

Ao, Y., Wang, Q., and Chen, P., (2002), "Simulating the Worn Surface in a Wear Process," Wear, Vol. 252, pp. 37-47.

Barber, J. R. and Ciavarella, M., (2000): "Contact Mechanics," *International Journal of Solids and Structures*, 37, pp. 29-43.

Borodich, F. M.; Onishchenko, D. A. (1997): "Multilevel Profile with Heirarchical Structure: Self-Affinity, Fractality and Applications to Contact Problems," Department of Mathematics, Glasgow Caledonian University Report TR/MAT 97-85.

Carslaw, H.S., and Jaeger, J.C., (1959): *Conduction of Heat in Solids*, Oxford University Press, London.

Choi, J., and Bryant, M.D., (2002): "Combining Lumped Parameter Bond Graphs with Finite Element Shafts in a Gearbox Model," *CMES: Computer Modeling in Engineering & Sciences*, Vol. 3, Num. 4, pp. 431-446.

Christensen, H., "Stochastic Models for Hydrodynamic Lubrication of Rough Surfaces," *Proc Instn Mech Engrs*, 1969-70; 184 (Part 1, 55): 1013-1026 (1970).

Greenwood, J.A., and Tripp, J.H., (1971): "The Contact of Two Nominally Flat Rough Surfaces," *Proc. Instn. Mech. Engrs*, 185, pp.48-71.

Greenwood, J.A., and Williamson, J.B.P., (1966): "Contact of Nominally Flat Surface," *Proc. Roy. Soc*., **A295**, pp.300-319.

Hu, Y.Z., and Tonder, K., (1992): "Simulation of 3-D Random Surface by 2-D Digital Filter and Fourier Analysis," *Int. Journal of Mach. Tool Manufact*, **32**, pp.82-90.

Hu, Y., Liu, Y., and **Wang, H.**: (2002): "Simulations of Scuffing Based on a Dynamic System Model," *CMES: Computer Modeling in Engineering & Sciences*, Vol. 3, Num. 4, pp. 447-454.

Huang, J.H., and Ju, F.D., (1985): "Thermomechanical Cracking Due to Moving Frictional Loads," *Wear*, 102, pp. 81-104.

Ioannides, E., and Harris, T.A., (1985): "A new fatigue life model for rolling bearings," *ASME Journal of Tribology* **107**, 367.

Jang, J.Y. and Khonsari, M., (2002): "Thermohydrodynamic Analysis of Journal Bearings Lubricated with Multigrade Oils," *CMES: Computer Modeling in Engineering & Sciences*, Vol. 3, Num. 4, pp. 455-464.

Johnson, K.L., (1996), *Contact Mechanics*, Cambridge University Press.

Ju, Y. and Farris, T.N., (1996): "Spectral Analysis of Two-Dimensional Contact problems," *ASME Journal of Tribology*, **118,** pp.320-328.

Lubrecht, A. A. and Ioannides, E. (1991): "A Fast Solution of the Dry Contact Problem and the Associated Subsurface Stress-Field Using Multilevel Techniques." *J Tribol*, **113,** pp. 128-133.

Karnopp, D.C., Margolis, D.L., and Rosenberg, R.C., (2000): *System Dynamics, a Unified Approach*, 3rd edition, Wiley, New York.

Ling, F.F., (1973): *Surface Mechanics, John Wiley & Sons*, New York.

Liu, G., Wang, Q., and Lin, C., (1999): "A survey of Current Models for Simulating the Contact Between Rough Surfaces," *Tribology Transaction*, **42** (3), pp. 581-591.

Liu, S.B., Wang, Q., and, Liu, G., (2000): "A Versatile Method of Discrete Convolution and FFT (DC-FFT) for Contact Analyses," *Wear*.

Liu, S.B., Wang, Q.J., Rodgers, M.J., Keer, L.M., and Cheng, H.S., (2002 "Temperature Distributions and Thermoelastic Displacements in Moving Bodies," *CMES: Computer Modeling in Engineering & Sciences*, Vol. 3, Num. 4, pp. 465-481.

Liu, S.B., and Wang, Q., (2001): "A Three-Dimensional Thermomechanical Model of Contact Between Non-Conforming Rough Surfaces," *ASME Journal of Tribology*, 123, pp. 17-26 (2001).

Majumdar, A.; Bhusan, B. (1991): "Fractal Model of Elastic-Plastic Contact Between Rough Surfaces" *ASME Journal of Tribology* **113**, 1-11.

Murakami, Y.,Sakae, Ichimaru, K., and Morita, T., (1997): "Experimental and fracture mechanics study of the pit formation mechanism under repeated lubricated rolling-sliding contact: Effects of reversal of rotation and

change of the driving roller," *ASME Journal of Tribology* **119**, 788.

Nogi, T., and Kato, T., (1997): "Influence of a Hard Surface Layer on the Limit of Elastic Contact-Part I: Analysis Using a Real Surface Model," *ASME Journal of Tribology*, **119**, pp.493-500.

Patir, N., (1978): " A Numerical Procedure for Random Generation of Rough Surfaces," *Wear*, **47**, pp.263-277.

Patir, N., and Cheng, H.S., (1978): "An Average Flow Model for Determining Effects of Three-Dimensional Roughness on Partial Hydrodynamic Lubrication," *Journal of Lubrication Technology*, Vol. 100, pp. 12-17.

Paynter, H.M., (1960): *Analysis and Design of Engineering Systems*, MIT Press: Cambridge, Mass.

Pinkus, O., (1990): *Thermal Aspects of Fluid Film Tribology*, ASME Press.

Pinkus, O., and Sternlicht, B., (1961). *Theory of Hydrodynamic Lubrication*,"McGraw-Hill, Inc.

Polonsky, I. A.; Keer, L. M. (1999): "A new numerical method for solving rough contact problems based on the multi-level multi-summation and conjugate gradient technique." *Wear*, vol. 231, pp. 206-219.

Polonsky, I.A., and Keer, L.M., (2000a): "A Fast and Accurate Method for Numerical Analysis of Elastic Layered Contacts," *ASME Journal of Tribology*, **122**, pp.30-35.

Polonsky, I.A., and Keer, L.M., (2000b): "Fast Methods for Solving Rough Contact Problems: A Comparative Study," *ASME Journal of Tribology*, **122**, pp.36-41.

Polonsky, I.A. and Keer, L.M., (2001): "Stress Analysis of Layered Elastic Solids with Cracks Using the Fast Fourier Transform and Conjugate Gradient Techniques," *Journal of Applied Mechanics*, Vol., 68.

Polonsky, I.A. and Keer, L.M., (2002): "Numerical Analysis of the Effect of Coating Microstructure on Three-Dimensional Crack Propagation of the Coating Under Rolling Contact Fatigtue Consitions," *Journal of Tribology*, Vol. 124, pp. 14-19.

Rodgers, M.J., Keer, L.M., and Cheng, H.S., (2002): "Steady-State Temperature Rise in a Coated Halfplanes," *CMES: Computer Modeling in Engineering & Sciences*, Vol. 3, Num. 4, pp. 483-495.

Sainsot, P., Jacq, C., and Nélias, D, (2002): "A Numerical Model for Elastoplastic Rough Contact," *CMES: Computer Modeling in Engineering & Sciences*, Vol. 3, Num. 4, pp. 497-506.

Shi, F., and Paranjpe, R., (2002): "An Implicit Finite Element Cavitation Algorithm," *CMES: Computer Modeling in Engineering & Sciences*, Vol. 3, Num. 4, pp. 507-515.

Tichy, J. A. and Meyer, M., (2000): "Review of Solid Mechanics in Tribology," *International Journal of Solids and Structures*, **37**, pp. 391-400.

Timoshenko, S. P., and Goodier, J. N., (1970): *Theory of Elasticity*, 3rd edition, McGraw-Hill, New York

Ting, B.Y., and Winer, W.O., (1989): "Frictional-Induced Thermal Influences in Elastic Contact Between Spherical Asperities," *ASME Journal of Tribology*, **111**, pp.315-322.

Voevodin, A.A., and Zabinski, J.S., (1998): "Load-adaptive crystalline-amorphous nanocomposites," *Journal of Materials Science* **33**, 319.

Wang, Y., Wang, Q., and Lin, C., (2002): "Mixed Lubrication of Coupled Journal-thrust Bearing Systems," *CMES: Computer Modeling in Engineering & Sciences*, Vol. 3, Num. 4, pp. 517-530.

Way, S., (1935): "Pitting due to rolling contact," *ASME Journal of Applied Mechanics* **2**, A49.

Whitehouse, D.J., and Archard, J.F., (1970): "The Properties of Random Surfaces of Significance in Their Contact," *Proc. Roy. Soc. Lond*, **A316**, pp.97-121.

Woodward, W. and Paul, B., (1976): "Contact Stress for Closely Conforming Bodies - Application to Cylinders and spheres," DOT-TST-77-48, Government Publications, Department of Transportation, Washington, D. C.

Zaretsky, E.V., Poplawski, J.V., and Peters, S.M., (1996): "Comparison of life theories for rolling-element bearings," *STLE Tribology Transactions* **39**, 237.

Zhu, D., and Hu, Y.Z., (2001): "A Computer Program Package for the Prediction of EHL and Mixed Lubrication Characteristics, Friction, Subsurface Stresses and Flash Temperatures Based on Measured 3-D Surface Roughness," *Tribologyy Transactions* **44**, pp.383-390